Kinetics and Mechanistic Aspects of As(III) Oxidation by Aqueous Chlorine, Chloramines, and Ozone: Relevance to Drinking Water Treatment

ARTICLE *in* ENVIRONMENTAL SCIENCE AND TECHNOLOGY · JUNE 2006

Impact Factor: 5.33 · DOI: 10.1021/es0524999 · Source: PubMed

9 AUTHORS, INCLUDING:

Adrian Ammann
Eawag: Das Wasserforschungs-Institut des E…
27 PUBLICATIONS **939** CITATIONS
SEE PROFILE

Pham Hung Viet
Vietnam National University, Hanoi
159 PUBLICATIONS **4,379** CITATIONS
SEE PROFILE

Ha Cao
University of Manitoba
2 PUBLICATIONS **86** CITATIONS
SEE PROFILE

Michael Berg
Eawag: Das Wasserforschungs-Institut des E…
101 PUBLICATIONS **4,314** CITATIONS
SEE PROFILE

Environ. Sci. Technol. **2006**, *40,* 3285−3292

Kinetics and Mechanistic Aspects of As(III) Oxidation by Aqueous Chlorine, Chloramines, and Ozone: Relevance to Drinking Water Treatment

MICHAEL C. DODD,[†] NGOC DUY VU,[‡] ADRIAN AMMANN,[†] VAN CHIEU LE,[‡] REINHARD KISSNER,[§] HUNG VIET PHAM,[‡] THE HA CAO,[‡] MICHAEL BERG,[†] AND URS VON GUNTEN*,[†]

Swiss Federal Institute of Aquatic Science and Technology (EAWAG), 8600 Duebendorf, Switzerland, Center for Environmental Technology and Sustainable Development (CETASD), Hanoi University of Science, Nguyen Trai Street 334, Hanoi, Vietnam, and Laboratory of Inorganic Chemistry, ETH Zurich, 8093 Zurich, Switzerland

Kinetics and mechanisms of As(III) oxidation by free available chlorine (FAC—the sum of HOCl and OCl^-), ozone (O_3), and monochloramine (NH_2Cl) were investigated in buffered reagent solutions. Each reaction was found to be first order in oxidant and in As(III), with 1:1 stoichiometry. FAC−As(III) and O_3−As(III) reactions were extremely fast, with pH-dependent, apparent second-order rate constants, k''_{app}, of 2.6 (±0.1) × 10^5 M^{-1} s^{-1} and 1.5 (±0.1) × 10^6 M^{-1} s^{-1} at pH 7, whereas the NH_2Cl−As(III) reaction was relatively slow (k''_{app} = 4.3 (±1.7) × 10^{-1} M^{-1} s^{-1} at pH 7). Experiments conducted in real water samples spiked with 50 μg/L As(III) (6.7 × 10^{-7} M) showed that a 0.1 mg/L Cl_2 (1.4 × 10^{-6} M) dose as FAC was sufficient to achieve depletion of As(III) to <1 μg/L As(III) within 10 s of oxidant addition to waters containing negligible NH_3 concentrations and DOC concentrations <2 mg-C/L. Even in a water containing 1 mg-N/L (7.1 × 10^{-5} M) as NH_3, >75% As(III) oxidation could be achieved within 10 s of dosing 1−2 mg/L Cl_2 (1.4−2.8 × 10^{-5} M) as FAC. As(III) residuals remaining in NH_3-containing waters 10 s after dosing FAC were slowly oxidized ($t_{1/2} \geq 4$ h) in the presence of NH_2Cl formed by the FAC−NH_3 reaction. Ozonation was sufficient to yield >99% depletion of 50 μg/L As(III) within 10 s of dosing 0.25 mg/L O_3 (5.2 × 10^{-6} M) to real waters containing <2 mg-C/L of DOC, while 0.8 mg/L O_3 (1.7 × 10^{-5} M) was sufficient for a water containing 5.4 mg-C/L of DOC. NH_3 had negligible effect on the efficiency of As(III) oxidation by O_3, due to the slow kinetics of the O_3−NH_3 reaction at circumneutral pH. Time-resolved measurements of As(III) loss during chlorination and ozonation of real waters were accurately modeled using the rate constants determined in this investigation.

Introduction

Arsenic is a common contaminant of groundwater resources around the world (*1*−*4*). Soluble inorganic arsenic occurs in surface waters and groundwaters primarily as a combination of arsenous acid (As(III)) and arsenic acid (As(V)) (*1*). The former state predominates under anoxic conditions (e.g., in oxygen-limited groundwaters), and the latter under oxic conditions (*1*), although As(III) can exist as a meta-stable species even in oxygen-rich environments, due to the slow kinetics of its oxidation by oxygen (*1*). Generally, dissolved arsenic occurs in groundwaters at concentrations <5 μg/L (*1, 2, 5*). However, in certain regions, including the western United States (*2, 6*) and southern Asia (*3, 4*), groundwaters utilized for drinking water often contain arsenic concentrations in substantial excess of the 10 μg/L guideline value recommended by the WHO (*5*) and adopted as a regulatory limit by the EU (*7*) and USEPA (*8*).

When sufficient infrastructure is available, aqueous arsenic concentrations can be lowered to ≤ 10 μg/L by a variety of conventional drinking water treatment methods, though many of these methods remove As(III) substantially less efficiently than As(V) (*9*). In cases for which As(total) is constituted in large part by As(III), arsenic removal by such methods can be improved by preoxidizing As(III) to As(V) (*9*−*11*). However, oxidant-scavenging matrix constituents, such as dissolved organic matter (DOM) and NH_3 - which can be present at high concentrations within reduced, As-(III)-laden groundwaters (*3, 12, 13*), may impair As(III) oxidation efficiency by competing with As(III) for available oxidant (*10*). Quantitative knowledge of the rate constants and mechanisms governing oxidation of As(III) by common drinking water oxidants would greatly facilitate modeling and optimization of As(III) oxidation processes for treatment of such waters.

Apparent second-order rate constants, k''_{app}, were measured for oxidation of As(III) by FAC, NH_2Cl, and O_3 within the pH range 2 to 11, to permit evaluation of pH-dependencies for each reaction. Stoichiometries and reaction orders were also measured, to facilitate identification of probable oxidation mechanisms. Additional experiments were conducted in water samples collected from Lake Zurich in Switzerland, and from two groundwater treatment facilities in Hanoi, Vietnam, to quantify the effects of matrix composition on As(III) oxidation efficiency and to test the suitability of measured rate constants for modeling As(III) oxidation in real water systems.

Materials and Methods

Chemical Reagents. As(III) and As(V) stock solutions were prepared from $NaAsO_2$ (purity ≥99%) and $Na_2HAsO_4 \cdot 7H_2O$ (purity ≥98.5%) obtained from Fluka. FAC stock solutions were prepared from NaOCl (~7% available chlorine) obtained from Riedel-de Haën, and standardized by iodometric titration (*14*). Chloramine and O_3 stocks were prepared according to published procedures (*15, 16*). Additional reagents were commercially available and of at least reagent grade purity. All stock solutions were prepared in deionized water (ρ ≥ 18.2 MΩ−cm) obtained from a Millipore Milli-Q or Barnstead NANOpure water purifier. Fifty-mM As(III) stocks were prepared approximately bi-monthly, during which time they were stable to within 5% of their initial

* Corresponding author phone: +41 44 823 52 70; fax: +41 44 823 52 10; e-mail: vongunten@eawag.ch.
[†] Swiss Federal Institute of Aquatic Science and Technology (EAWAG).
[‡] Hanoi University of Science.
[§] Laboratory of Inorganic Chemistry, ETH Zurich.

10.1021/es0524999 CCC: $33.50
Published on Web 04/15/2006

TABLE 1. Experimental Approaches Used for Rate Constant Measurements and Real Water Experiments

experiment (method)[a]	T (°C)	measurement endpoint[e]	experimental matrix(es)[f,g]	quenching agent(s)[g]
NH_2Cl kinetics (batch[b])	25 (±0.5)	NH_2Cl loss (measured at $\lambda = 243$ nm)	buffered As(III) stock	NA
$NHCl_2$ kinetics (batch[b])	25 (±0.5)	$NHCl_2$ loss (measured at $\lambda = 310$ nm)	buffered As(III) stock	NA
FAC kinetics (CFL[b])	23 (±2)[d]	FAC loss (measured via DPD method)	buffered As(III) stock (C1), buffered FAC stock (C2)	DPD (C3)
O_3 kinetics (CFL[b])	23 (±2)[d]	O_3 loss (measured via indigo method)	buffered As(III) stock (C1), pH 4 O_3 stock (C2)	indigo (C3)
O_3 kinetics (SFL[b])	20 (±0.5)	O_3 loss (measured at $\lambda = 258$ nm)	buffered As(III) stock (C1), buffered O_3 stock (C2)	NA
real water chlorination (batch[c])	25 (±0.5)	measurement of As(III) loss for various FAC doses	As(III)-spiked real water	ascorbic acid or DPD[i]
real water chlorination (batch[c])	25 (±0.5)	measurement of As(III) loss in the presence of various NH_2Cl concentrations	As(III)-spiked real water	ascorbic acid or DPD[i]
real water ozonation (batch[c])	20 (±0.5)	measurement of As(III) loss for various O_3 doses	As(III)-spiked real water	none
real water chlorination (CFL[c])	23 (±2)[d]	time-resolved monitoring of As(III) loss for an applied excess of FAC	As(III)-spiked real water (C1), buffered FAC stock (C2)	ascorbic acid or DPD (C3)[i]
real water ozonation (CFL[c])	23 (±2)[d]	time-resolved monitoring of As(III) loss for an applied excess of O_3	As(III)-spiked real water (C1), pH 4 O_3 stock (C2a), buffer (C2b)[h]	cinnamic acid (C3)[j]

[a] CFL-continuous-flow, SFL-stopped-flow. [b] Experimental details included in the Supporting Information, Text S2. [c] Experimental details included in the Supporting Information, Text S5. [d] Room temperature. [e] Reaction kinetics experiments conducted with As(III) in large excess of each oxidant. Real water experiments conducted at starting concentrations of 50 μg/L As(III) (6.7×10^{-7} M). [f] Phosphate, acetate, and borate buffers adjusted to desired pH values in reaction kinetics experiments or, in real water experiments, to the appropriate real water's native pH. O_3 stocks acidified to pH 4 by dropwise addition of 150 mM sulfuric acid. [g] As(III)-containing solutions introduced on channel 1 (C1) of the CFL system, oxidant solutions on channel 2 (C2), and quenching reagent solutions on channel 3 (C3). [h] O_3 stock (C2a) and buffer (C2b) premixed to yield a buffered O_3 stock (C2) at the real water pH immediately prior to further mixing with As(III)-spiked real water (C1). [i] Ascorbic acid used to quench samples intended for As(III) analyses and DPD used to monitor FAC residuals. [j] The O_3-cinnamic acid reaction yields benzaldehyde in 1:1 stoichiometry (*17*). Residual O_3 concentrations were calculated from benzaldehyde concentrations in quenched samples.

TABLE 2. Water Sources and Important Parametric Measurements[a]

water	pH	DOC, mg-C/L	alkalinity, mM HCO_3^-	NH_3, mg-N/L (mol-N/L)
Lake Zurich (LZ)	8.0	1.5−1.6	2.6−2.7	<0.01 ($<7.1 \times 10^{-7}$)
Lake Zurich (LZ1)[b]	8.0	1.5−1.6	2.6−2.7	1 (7.1×10^{-5})
Lake Zurich (LZ20)[b]	8.0	1.5−1.6	2.6−2.7	20 (1.4×10^{-3})
Phap Van (PV)	7.3	5.3−5.4	5.1−5.2	20−25 ($1.4-1.8 \times 10^{-3}$)
Yen Phu (YP)	7.2	1.1	2.1−2.9	<0.01 ($<7.1 \times 10^{-7}$)

[a] Multiple samples of each water, collected on different dates over a four-month time-span, were utilized to conduct the real water experiments described herein; thus, ranges of measurements are provided for each water quality parameter. Single values indicate that measurements were the same for each sample. [b] Separate aliquots of native LZ water were amended with NH_4Cl (LZ1 with 1 mg-N/L (7.1×10^{-5} M), and LZ20 with 20 mg-N/L (1.4×10^{-3} M)) for use in batch and time-resolved chlorination experiments.

concentration. Working As(III) solutions were prepared from these stocks before each experiment. Aluminosilicate adsorbent for the separation of As(III) and As(V) (described in detail in the Supporting Information, Text S1), was purchased from Dr. Xiaoguang Meng, Stevens Institute of Technology, Hoboken, NJ.

Analytical Methods. As(III) and As(V) concentrations were measured by ion-chromatography/ICP−MS (see Supporting Information, Text S1 for details). *p*-Chlorobenzoic acid (*p*CBA) and benzaldehyde analyses were performed by HPLC−UV (Text S1).

Determination of Rate Constants. Rate constants for the reactions of As(III) with FAC, NH_2Cl, $NHCl_2$, and O_3, were measured by various techniques selected according to reactant characteristics and reaction rates. In each case, oxidant consumption was measured in the presence of a large excess of As(III), to maintain pseudo-first-order conditions with respect to oxidant. Individual experimental procedures are summarized in Table 1 and described in detail within Text S2.

Stoichiometric Measurements. Stoichiometries of the reactions between As(III) and each oxidant (excluding $NHCl_2$) were measured with either As(III) or the oxidant in excess. In each case, increasing concentrations of the limiting reactant were dosed under constant, rapid stirring to buffered solutions of the reactant-in-excess. Reactions were allowed to proceed for time intervals sufficient to ensure complete consumption of the limiting reactant, prior to sampling and analysis for the reactant-in-excess. When As(III) was dosed to solutions containing excess O_3, experiments were conducted under gastight conditions to minimize evaporative O_3 losses (details in Text S3).

Real Water Experiments. Water samples used for real water experiments are listed with corresponding water quality parameters in Table 2. These waters, which contained native As(III) concentrations <2 μg/L, were spiked with 50 μg/L As(III) for experiments. Separate aliquots of Lake Zurich water were spiked with 1 or 20 mg-N/L (7.1×10^{-5} or 1.4×10^{-3} M) as NH_3 to simulate waters containing high NH_3 and low DOC concentrations. Sample procurement details and source water descriptions are provided in Text S4. Methods utilized for real water experiments are summarized in Table 1, and described in detail within Text S5.

Results and Discussion

As(III) Oxidation Kinetics. Pseudo-first-order rate constants, k'_{obs}, were obtained for reactions of As(III) with each oxidant by linear regression of plots of ln([Oxidant]) versus time, or by exponential regression of plots of [Oxidant] versus time, where appropriate (details are provided in the Supporting

Information—Part B). As(III) reaction orders were determined by evaluating the dependence of k'_{obs} on [As(III)] for each reaction. Plots of $\log(k'_{obs})$ v. $\log([As(III)])$ for FAC, NH_2Cl, and O_3 reactions all yielded slopes of 1.0 (±0.07) (Figure S1), indicating that each reaction can be treated as first-order with respect to As(III). The reactions of As(III) with FAC, NH_2Cl, and O_3 could thus be described by a second-order kinetic model (eq 1),

$$\frac{d([As(III)])}{dt} = \frac{d([Ox])}{dt} = -k''_{app}[As(III)]\,[Ox] = -k'_{obs}[Ox] \quad (1)$$

where k''_{app} (calculated by dividing k'_{obs} by [As(III)]) represents the pH-dependent, apparent second-order rate constant at a particular pH. In contrast to its reactions with the other oxidants, As(III) was found to react with $NHCl_2$ with an order of 0.7 (Figure S1).

Free Available Chlorine. Figure 1a, which shows the magnitude of $k''_{app,FAC}$ at various pH values, illustrates that As(III) reacts very rapidly with FAC. $k''_{app,FAC}$ is 2.6 (±0.1) × 10^5 M^{-1} s^{-1} at pH 7, corresponding to a $t_{1/2,As(III)}$ of 95 ms in the presence of 2 mg/L Cl_2 (2.8×10^{-5} M) as FAC. The pH-dependency of $k''_{app,FAC}$ can be attributed to varying contributions of each reactant's acid–base species to apparent FAC–As(III) reactivity.

$As(OH)_3$ dissociates in aqueous solution according to eqs 2–4 (*18*).

$$As(OH)_3 \overset{K_{a1}}{\rightleftharpoons} As(OH)_2O^- + H^+ \quad pK_{a1} = 9.2 \quad (2)$$

$$As(OH)_2O^- \overset{K_{a2}}{\rightleftharpoons} As(OH)O_2^{2-} + H^+ \quad pK_{a2} = 12.1 \quad (3)$$

$$As(OH)O_2^{2-} \overset{K_{a3}}{\rightleftharpoons} AsO_3^{3-} + H^+ \quad pK_{a3} = 12.7 \quad (4)$$

At circumneutral pH, $As(OH)_3$ represents the most abundant As(III) species. A small fraction (up to ~0.1) of As(III) is present as $As(OH)_2O^-$ under these conditions, and very small fractions (<5×10^{-6}) are present as $As(OH)O_2^{2-}$ and AsO_3^{3-} (Figure 1a). FAC speciation can be described by eq 5 (*19*).

$$HOCl \overset{K_a}{\rightleftharpoons} OCl^- + H^+ \quad pK_a = 7.4 \quad (5)$$

FAC–As(III) reaction kinetics can be characterized according to eight possible reactions between the four As(III) species (eqs 2–4) and two FAC species (eq 5), by incorporating species distribution terms into eq 1 and rearranging to yield eq 6,

$$k''_{app,FAC} = \sum_{\substack{i=1,2 \\ j=1,2,3,4}} \frac{k''_{ij}\,\alpha_i[FAC]\,\beta_j[As(III)]}{[FAC]\,[As(III)]} = \sum_{\substack{i=1,2 \\ j=1,2,3,4}} k''_{ij}\,\alpha_i\,\beta_j \quad (6)$$

where α_i and β_j represent the respective fractions of oxidant and substrate present as the species i and j at a given pH (*20*), and k''_{ij} represents the specific second-order rate constant for each i and j pair.

The increase in magnitude of $k''_{app,FAC}$ up to pH 8.3 can be attributed primarily to an increase in the fraction of As(III) present as $As(OH)_2O^-$, which is expected to be a stronger nucleophile than $As(OH)_3$. The decrease in magnitude of $k''_{app,FAC}$ above pH 8.3 can be attributed to an accompanying decrease in proportion of HOCl relative to OCl^-, which is a much weaker oxidant than HOCl (*15, 21–23*). Consequently, the magnitude of $k''_{app,FAC}$ is highest near pH 8.3 (the average of $pK_{a1,As(III)}$ and $pK_{a,HOCl}$), where the product $\alpha_{HOCl}\beta_{As(OH)_2O^-}$ ($\alpha_1\beta_2$) reaches a maximum (Figure 1a). These observations indicate that OCl^- reactions are unimportant relative to HOCl reactions within the pH range studied. Therefore, the magnitude of $k''_{app,FAC}$ is governed primarily by the reactions of HOCl with each acid–base species of $As(OH)_3$. $k''_{app,FAC}$ can thus be modeled by neglecting OCl^- reactions.

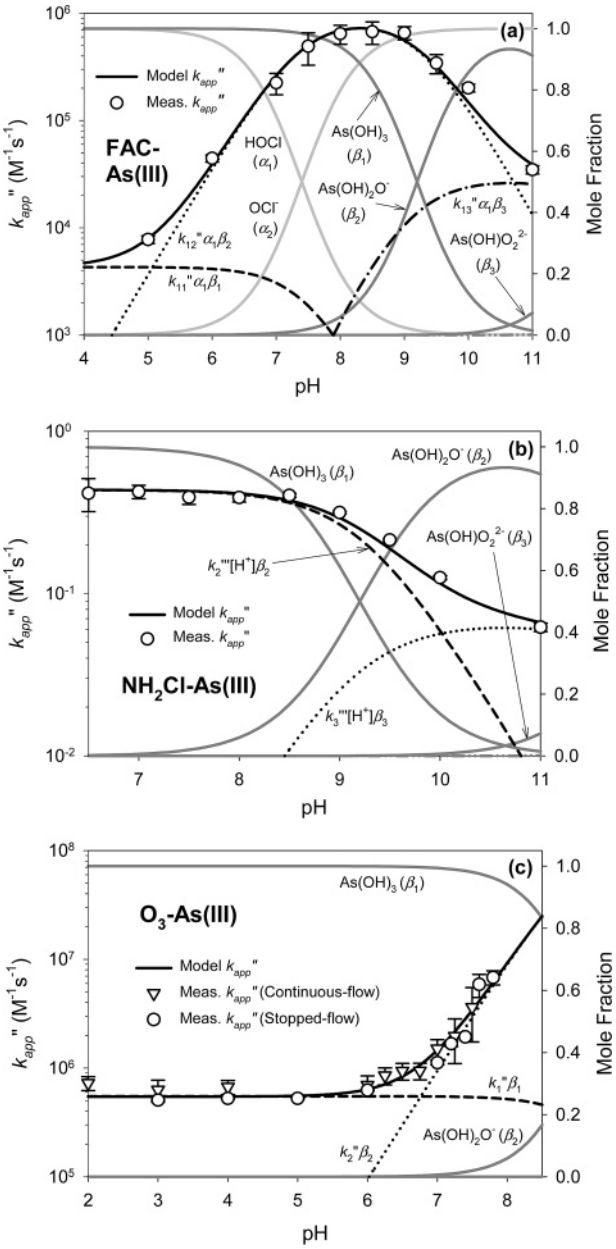

FIGURE 1. Apparent second-order rate constants for As(III) oxidation by (a) FAC, (b) NH_2Cl, and (c) O_3. FAC experiments conducted at [As(III)] = 15–50 × 10^{-6} M, $[FAC]_0$ = 1.5–5 × 10^{-6} M, and 23 (±2) °C, NH_2Cl experiments at [As(III)] = 5 × 10^{-3} M, $[NH_2Cl]_0$ = 2 × 10^{-4} M, and 25 (±0.5) °C, and O_3 experiments at [As(III)] = 10–200 × 10^{-6} M, $[O_3]_0$ = 1–10 × 10^{-6} M, and 23 (±2) °C (CFL) or 20 (±0.5) °C (SFL).

Specific rate constants, k''_{1j} – calculated by nonlinear regression of measured $k''_{app,FAC}$ values, according to eq 6 (via SigmaPlot 2002, SPSS software), are summarized in Table 3. The model fit shown in Figure 1a, which was obtained by using these k''_{1j} values, demonstrates the accuracy of eq 6 in describing measured magnitudes of $k''_{app,FAC}$. k''_{14} could not be accurately determined from available data. However, this term is unimportant within the pH range studied, as HOCl–As(III) reactivity is governed almost exclusively by k''_{11}, k''_{12}, and k''_{13} under these conditions (Figure 1a).

Chloramines. The magnitude of k''_{app,NH_2Cl} is shown at various pH values in Figure 1b. These data illustrate that

TABLE 3. Specific Rate Constants Determined for Reactions of As(III) with HOCl, NH_2Cl, and O_3

oxidant	substrate	specific rate constant	k''_{app} (M^{-1} s^{-1}), pH 7 ($t_{1/2}$ at 2 mg/L oxidant concentration)[b]
HOCl	$As(OH)_3$	$k''_{11} = 4.3\ (\pm0.8) \times 10^3\ M^{-1}\ s^{-1}$	$2.6\ (\pm0.1) \times 10^5$ ($t_{1/2}$ = 95 ms)
	$As(OH)_2O^-$	$k''_{12} = 5.8\ (\pm0.1) \times 10^7\ M^{-1}\ s^{-1}$	
	$As(OH)O_2^{2-}$	$k''_{13} = 1.4\ (\pm0.1) \times 10^9\ M^{-1}\ s^{-1}$	
NH_2Cl	$As(OH)_2O^-$	k'''_2[a] $= 6.9\ (\pm2.7) \times 10^8\ M^{-2}\ s^{-1}$	$4.3\ (\pm1.7) \times 10^{-1}$ ($t_{1/2}$ = 16 h)
	$As(OH)O_2^{2-}$	k'''_3[a] $= 8.3\ (\pm7.8) \times 10^{10}\ M^{-2}\ s^{-1}$	
O_3	$As(OH)_3$	$k''_1 = 5.5\ (\pm0.1) \times 10^5\ M^{-1}\ s^{-1}$	$1.5\ (\pm0.1) \times 10^6$ ($t_{1/2}$ = 11 ms)
	$As(OH)_2O^-$	$k''_2 = 1.5\ (\pm0.1) \times 10^8\ M^{-1}\ s^{-1}$	

[a] Third-order, H^+-catalysis rate constant. [b] calculated for pseudo-first-order conditions of excess oxidant, assuming 2 mg/L concentrations of FAC (28 μM), NH_2Cl (28 μM), and O_3 (42 μM).

As(III) reacts relatively slowly with NH_2Cl. k''_{app,NH_2Cl} is 4.3 (±1.7) $\times 10^{-1}\ M^{-1}\ s^{-1}$ at pH 7, corresponding to a $t_{1/2,As(III)}$ of 16 h in the presence of 2 mg/L Cl_2 (2.8×10^{-5} M) as NH_2Cl. The inverse relationship between pH and magnitude of k''_{app,NH_2Cl} from pH 8 to 11 (Figure 1b) is suggestive of acid-catalysis, in analogy to the reactions of NH_2Cl with SO_3^{2-} (*24*), NO_2^- (*25*), and I^- (*15*). This catalysis appears to be H^+-specific, as k''_{app,NH_2Cl} exhibited no measurable dependence on phosphate (50−182 mM) or borate (10−80 mM) concentrations.

The plateau in magnitude of k''_{app,NH_2Cl} below pH 8 indicates that NH_2Cl−As(III) reaction kinetics are not significantly influenced by neutral $As(OH)_3$ within the pH range studied, because H^+-catalyzed oxidation of $As(OH)_3$ would require that the magnitude of k''_{app,NH_2Cl} increase continuously with increasing acidity. The trends in Figure 1b can, therefore, be attributed to H^+-catalyzed reactions of NH_2Cl with one or more anionic As(III) species, according to eq 7,

$$k''_{app,NH_2Cl} = [H^+] \sum_{j=2,3,4} k'''_j \beta_j \quad (7)$$

where k'''_j represents the respective third-order H^+-catalysis rate constants for each of the three anionic As(III) species, *j*. In the context of eq 7, the data in Figure 1b also suggest that the magnitude of k''_{app,NH_2Cl} is governed primarily by $As(OH)_2O^-$ below pH 8. Under these conditions, each successive unit decrease in pH is offset by an order of magnitude decrease in the mole fraction of $As(OH)_2O^-$, resulting in a constant value for the product of the $[H^+]$ and β_j terms in eq 7. This should, in turn, lead to a constant value of k''_{app,NH_2Cl}, assuming that $As(OH)O_2^{2-}$ and AsO_3^{3-} have minimal influence on reaction kinetics below pH 8.

These inferences were tested by nonlinear regression of measured k''_{app,NH_2Cl} values according to eq 7. The resulting model fit, obtained with the $k'''_{As(OH)_2O^-}$ and $k'''_{As(OH)O_2^{2-}}$ values listed in Table 3, is shown in Figure 1b. $k'''_{AsO_3^{3-}}$ could not be accurately determined, due to lack of data above pH 11. However, this term is unimportant within the pH range studied, as the magnitude of k''_{app,NH_2Cl} is clearly influenced primarily by $k'''_{As(OH)_2O^-}$ and $k'''_{As(OH)O_2^{2-}}$ between pH 6.5 and 11 (Figure 1b).

An Arrhenius plot of k''_{app,NH_2Cl} from 10 to 30 °C showed that E_a for the As(III)−NH_2Cl reaction is 27 (±2) kJ/mol (Supporting Information, Figure S2). A temperature change of 10 °C will, therefore, result in variation of k''_{app,NH_2Cl} by a factor of 1.4−1.5 within temperature ranges relevant to drinking water treatment.

$NHCl_2$−As(III) reaction kinetics were found to be far slower than NH_2Cl−As(III) kinetics. $k'_{obs,NHCl_2}$ increased from 0.4×10^{-5} to $2.4 \times 10^{-5}\ s^{-1}$ (i.e., $t_{1/2}$ = 8−48 h) in the presence of 13 mM of As(III), as pH decreased from 4 to 5 (Supporting Information, Figure S3). These data indicate that the reaction of As(III) with $NHCl_2$ can be neglected under typical drinking water disinfection conditions.

Ozone. The magnitude of k''_{app,O_3}, measured by CFL and SFL methods, is shown as a function of pH in Figure 1c. As illustrated by these data, As(III) reacts extremely rapidly with O_3. k''_{app,O_3} is 1.5 (±0.1) $\times 10^6\ M^{-1}\ s^{-1}$ at pH 7, corresponding to a $t_{1/2,As(III)}$ of 11 ms in the presence of 2 mg/L O_3 (4.2×10^{-5} M). The magnitude of k''_{app,O_3} is also strongly pH-dependent. However, oxidant speciation does not need to be considered for O_3 reactions, so k''_{app,O_3} can be characterized according to As(III) speciation alone. The constancy of k''_{app,O_3} below pH 6 can be attributed to the O_3−$As(OH)_3$ reaction, whereas the increase in k''_{app,O_3} above pH 6 can be attributed primarily to the O_3−$As(OH)_2O^-$ reaction. $As(OH)O_2^{2-}$ and AsO_3^{3-} exert negligible influence on the magnitude of k''_{app,O_3} below pH 8.5, since molar fractions of these two species are very small under such conditions ($< 5 \times 10^{-6}$).

k''_j values were determined for the O_3−As(III) reaction by fitting eq 6 to k''_{app,O_3} in the same manner as for the As(III)−FAC reaction (with O_3 terms substituted for FAC terms). The resulting model fit, obtained with the $k''_{As(OH)_3}$ and $k''_{As(OH)_2O^-}$ values listed in Table 3, is shown in Figure 1c. $k''_{As(OH)O_2^{2-}}$ and $k''_{AsO_3^{3-}}$ could not be accurately determined from available data. However, the importance of these terms is negligible within the pH range studied, as apparent from the nearly exclusive dependence of k''_{app,O_3} on $k''_{As(OH)_3}$ and $k''_{As(OH)_2O^-}$ under these conditions (Figure 1c).

Mechanistic Considerations. As mentioned above, the FAC, NH_2Cl, and O_3 reactions were found to be first-order with respect to As(III) and oxidant (Figure S1). In addition, stoichiometries of As(III) oxidation by FAC, NH_2Cl, and O_3 were found to be 1:1 for all three reactions; that is, one mole of As(III) was consumed for each mole of oxidant consumed, whether experiments were conducted with As(III) or oxidant in excess (Supporting Information, Figure S4). Experiments conducted with As(III) in excess also verified that one mole of As(V) is produced for every mole of As(III) consumed (Figure S4).

Free Available Chlorine. On the basis of reaction order and stoichiometry, the oxidation of $As(OH)_3$ by HOCl, yielding $AsO(OH)_3$, superficially resembles a direct oxygen transfer reaction. O-transfer would involve direct nucleophilic substitution by As(III) at the oxygen atom in HOCl, with HCl as a leaving group. However, comparison with FAC reaction systems involving other inorganic nucleophiles (e.g., SO_3^{2-}, Br^-, I^-, CN^- (*22*)) suggests that As(III) oxidation more likely proceeds via initial Cl^+-transfer from HOCl to the As atom, with concomitant loss of OH^- (a much more favorable leaving group than HCl), to yield a transient $As(III)Cl^+$ intermediate that hydrolyzes to Cl^- and As(V) (eqs 8 and 9). This pathway is expected to apply to HOCl reactions with all four As(III) species.

$$HOCl + As(OH)_3 \xrightarrow{k''_{HOCl,As(OH)_3}} Cl^+As(OH)_3 + OH^- \quad (8)$$

$$Cl^{+}As(OH)_3 + H_2O \xrightarrow{k'_{Cl^{+}As(OH)_3}} AsO(OH)_3 + 2H^{+} + Cl^{-} \quad (9)$$

Monochloramine. NH_2Cl is known to react with a number of inorganic nucleophiles (e.g., SO_3^{2-}, NO_2^{-}, I^{-}) by acid-catalyzed Cl^{+}-transfer, to yield the same chloro-intermediates produced in corresponding FAC reactions (*15, 24, 25*). The order and 1:1 stoichiometry of the NH_2Cl−As(III) reaction, together with the pH-dependence of k''_{app,NH_2Cl}, are consistent with a similar mechanism (eq 10), which should apply to oxidation of all three anionic As(III) species. The chloro-intermediate formed in eq 10 would hydrolyze in analogy to eq 9.

$$H^{+} + NH_2Cl + As(OH)_2O^{-} \xrightarrow{k'''_{H^{+},NH_2Cl,As(OH)_2O^{-}}} Cl^{+}As(OH)_2O^{-} + NH_3 \quad (10)$$

Ozone. O_3 generally reacts with inorganic nucleophiles by two-electron processes involving O-transfer from O_3 to the nucleophile via a primary ozonide adduct, which decomposes to yield the oxidized substrate and O_2 (*26,27*). The order and 1:1 stoichiometry of the As(III)-O_3 reaction indicate that As(III) is similarly oxidized to As(V) by O-transfer from O_3 to the As atom (eqs 11 and 12). The same pathway is expected to apply to reactions of O_3 with all four As(III) species.

$$O_3 + As(OH)_3 \xrightarrow{k''_{O_3,As(OH)_3}} OOOAs(OH)_3 \quad (11)$$

$$OOOAs(OH)_3 \xrightarrow{k'_{OOOAs(OH)_3}} AsO(OH)_3 + O_2 \quad (12)$$

Oxidation of As(III) in Real Waters. *Chlorination—Free Available Chlorine Reactions.* Figure 2a depicts measured As(III) losses at various FAC doses in each of the real waters listed in Table 2. Fifty μg/L As(III) (6.7×10^{-7} M) was depleted to <1 μg/L As(III) by as little as 0.1 mg/L Cl_2 (1.4×10^{-6} M) as FAC during batch experiments conducted with LZ and YP waters (Figure 2a). Such high As(III) oxidation efficiency is consistent with the low DOC concentrations and lack of NH_3 in these two waters (Table 2). In contrast, As(III) oxidation efficiency was markedly suppressed in LZ1, LZ20, and PV waters (Figure 2a), due to rapid scavenging of FAC by the NH_3 present in the latter three waters ($k''_{app,FAC,NH_3} > 1 \times 10^4$ M^{-1} s^{-1} between pH 7 and 8 (*23*)).

Time-resolved As(III) losses during chlorination of LZ, LZ1, and YP waters were monitored by the CFL system mentioned in Table 1. Results obtained from these experiments are summarized in Figure 2b. FAC residuals were present during the monitored reaction periods in all three waters, ensuring rapid As(III) oxidation in each case. The higher rate of As(III) oxidation in LZ water, compared to YP water, can be attributed to the difference in pH of the two waters; with $k''_{app,FAC,As(III)} = 6.9 \times 10^5$ M^{-1} s^{-1} at pH 8 (LZ water), and 3.6×10^5 M^{-1} s^{-1} at pH 7.2 (YP water). Comparison of the results for LZ and LZ1 waters shows that As(III) oxidation efficiency was moderately impaired in the latter, due to rapid consumption of FAC by NH_3 (Figure 2b). These findings are consistent with the results obtained for batch experiments with the same waters (Figure 2a).

The As(III) losses shown in Figure 2b can be modeled with the rate constants reported in Table 3, by compensating for contemporaneous FAC loss to side-reactions with matrix constituents in each water. FAC losses were modeled according to pseudo-first-order rate "constants," $k'_{FAC,matrix}$, obtained from plots of ln([FAC]) vs time in each water. As(III) oxidation was in turn modeled by inserting the pseudo-first-order expression for FAC decay (eq 13) into a separate expression for As(III) oxidation (eq 14), and integrating to yield eq 15.

$$[FAC] = [FAC]_0\, e^{(-k'_{FAC,matrix}\, t)} \quad (13)$$

$$[As(III)] = [As(III)]_0\, e^{(-k''_{app,FAC}\int_0^t [FAC]dt)} \quad (14)$$

$$[As(III)] = [As(III)]_0 \exp\left(\frac{k''_{app,FAC}[FAC]_0}{k'_{FAC,matrix}}\left(e^{(-k'_{FAC,matrix}\, t)} - 1\right)\right) \quad (15)$$

The resulting model fits are shown as dotted lines in Figure 2b. The close agreement between model predictions and measured data for each real water demonstrates that one can accurately predict oxidation of As(III) by FAC in various real waters if the rate of FAC loss for a given water is known. However, in certain cases, one can make predictions of expected As(III) oxidation efficiencies even without directly measuring FAC loss rates. For example, FAC reacts with NH_3 far more rapidly than with DOM and most other matrix constituents; thus, in systems containing substantial NH_3 concentrations (e.g., >0.5 mg-N/L), FAC loss will likely be dominated by FAC−NH_3 reaction kinetics. In such cases, FAC loss can be predicted by modeling FAC consumption according to the second-order reaction between NH_3 and FAC. As(III) loss can in turn be modeled by substituting a second-order expression for FAC loss (eq 16) into eq 14 and integrating with respect to *t*, as described in the Supporting Information (Text S6), to yield eq 17.

$$[FAC] = \frac{[FAC]_0\left(1 - \frac{[NH_3]_0}{[FAC]_0}\right)}{\left(1 - \frac{[NH_3]_0}{[FAC]_0}\right) e^{(([NH_3]_0 - [FAC]_0)k''_{app,FAC,NH_3}\, t)}} \quad (16)$$

$$[As(III)] = [As(III)]_0 \exp\left(\frac{-k''_{app,FAC,As(III)}[FAC]_0\left(1 - \frac{[NH_3]_0}{[FAC]_0}\right)}{([NH_3]_0 - [FAC]_0)k''_{app,FAC,NH_3}} \times \left(\ln\left(\frac{e^{(([NH_3]_0 - [FAC]_0)k''_{app,FAC,NH_3}\, t)}}{\frac{[NH_3]_0}{[FAC]_0} e^{(([NH_3]_0 - [FAC]_0)k''_{app,FAC,NH_3}\, t)} - 1}\right) - \ln\left(\frac{1}{\frac{[NH_3]_0}{[FAC]_0} - 1}\right)\right)\right) \quad (17)$$

Model predictions obtained by eq 17 are compared with measurements from LZ1 water in Figure 2c. The model substantially over-predicted As(III) losses with respect to batch measurements. This was presumably a consequence of suboptimal mixing in the batch systems, which would have resulted in disproportionately large consumption of FAC by NH_3 during FAC dosage, in turn leading to lower As(III) loss than predicted for an ideally mixed system. However, model predictions correlated very well with CFL measurements (Figure 2c), consistent with the superior mixing efficiency achieved by the CFL system (i.e., FAC and real water solutions are mixed through a tee in 1:1 proportion during CFL experiments, as described in the Supporting Information, Text S2).

Chlorination—NH_2Cl Reactions. As(III) loss is expected to occur within two phases during chlorination of a water containing significant NH_3 concentrations: (i) initial, rapid oxidation of As(III) by FAC, and (ii) secondary, slow oxidation of As(III) in the presence of NH_2Cl generated by the FAC−NH_3 reaction, if insufficient FAC is added to completely oxidize As(III) during the first phase. As(III) losses measured

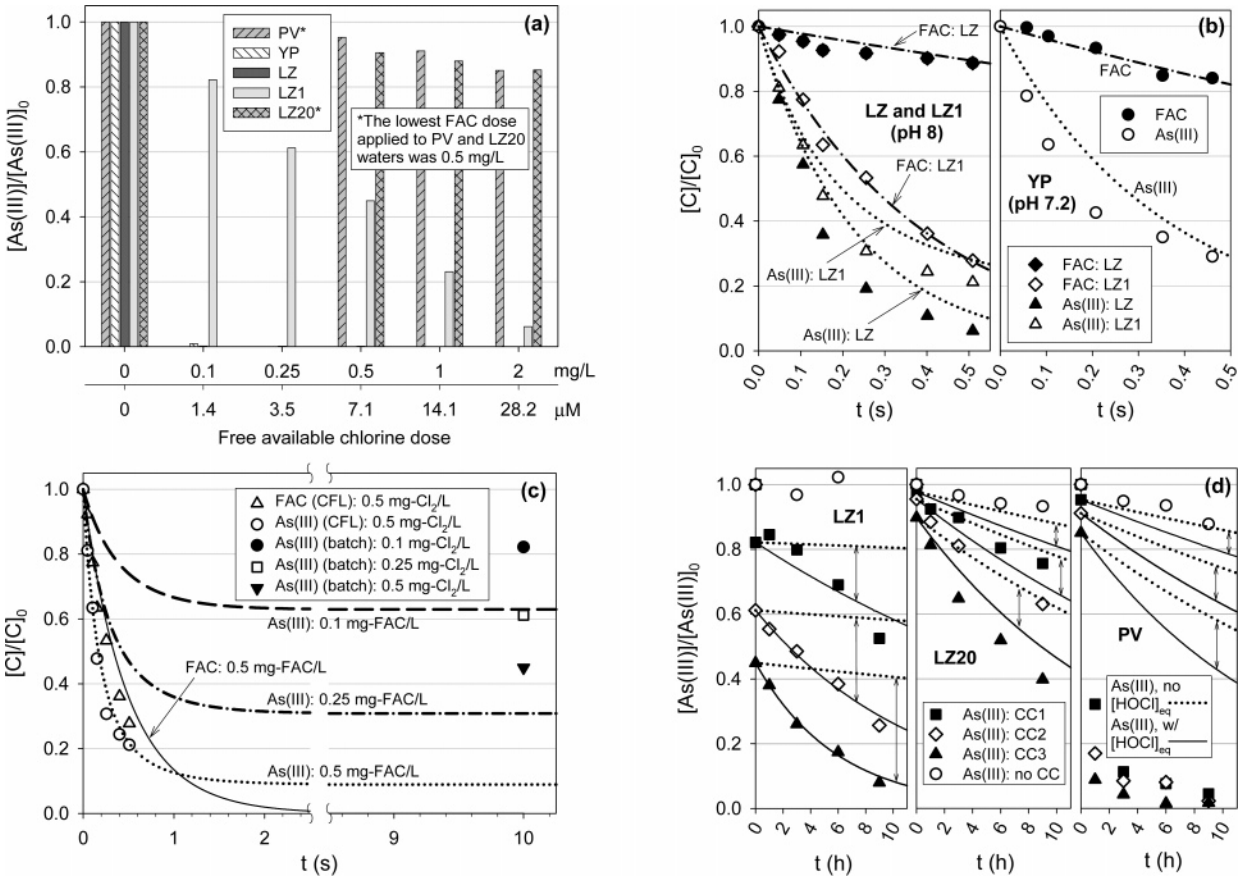

FIGURE 2. As(III) oxidation during chlorination of real waters spiked with 50 μg/L As(III) (6.7×10^{-7} M) (water quality data in Table 2). (a) As(III) loss 10 s after FAC addition to each real water, in batch at 25 ($\pm$0.5) °C, (b) time-resolved As(III) loss within LZ, LZ1, and YP waters for an applied FAC dose of 0.5 mg/L Cl_2 (7.1×10^{-5} M) at 23 ($\pm$2) °C, (c) comparison of As(III) losses measured within LZ1 water, in batch (25 ($\pm$0.5) °C) and by CFL (23 ($\pm$2) °C), with As(III) losses predicted for the same water by modeling FAC losses according to the second-order reaction between FAC and NH_3. (d) As(III) losses in LZ1, LZ20, and PV waters, in the presence of NH_2Cl formed from various FAC doses at 25 ($\pm$0.5) °C. CC1, CC2, and CC3 represent "combined chlorine" (i.e., NH_2Cl) concentrations of 0.1, 0.25, and 0.5 mg/L Cl_2 (1.4×10^{-6}, 3.5×10^{-6}, and 7.1×10^{-6} M) for LZ1 water, and 0.5, 1.0, and 1.8 mg/L Cl_2 (7.1×10^{-6}, 1.4×10^{-5}, and 2.5×10^{-5} M) for LZ20 and PV waters. DPD measurements verified that [NH_2Cl] did not decrease more than 10% during the total reaction times in any of these reaction solutions. Symbols in b–d refer to measurements, lines to model predictions.

within the latter phase, during chlorination of LZ1, LZ20, and PV waters, are shown in Figure 2d.

With the exception of LZ1 water dosed with 0.1 mg/L Cl_2 (1.4×10^{-6} M) as FAC, NH_2Cl concentrations in each water were in substantial excess of [As(III)], and remained essentially constant during monitored reaction periods in these waters (i.e., <10% change from $[NH_2Cl]_0$, data not shown). As(III) losses were, therefore, modeled initially by eq 18.

$$[\text{As(III)}] = [\text{As(III)}]_0 \, e^{(-k''_{\text{app},NH_2Cl}[NH_2Cl]\ t)} \quad (18)$$

However, this model substantially under-predicted the rate of As(III) loss observed within LZ1, LZ20, and PV waters (dotted lines in Figure 2d), presumably because it does not account for effects of the equilibrium between NH_2Cl and HOCl (eq 19) on As(III) oxidation.

$$NH_3 + HOCl \overset{K_{hyd}}{\rightleftharpoons} NH_2Cl + H_2O \quad (19)$$

The importance of eq 19 can be investigated by using the equilibrium constant, $K_{hyd} = 1.5 \times 10^{11}$ M^{-1} (*28*) to determine the equilibrium concentration, $[HOCl]_{eq}$, from known concentrations of NH_3 (Table 2) and NH_2Cl. $[FAC]_{eq}$ (including both HOCl and OCl^-) can then be calculated from $[HOCl]_{eq}$ and incorporated with $k''_{app,FAC}$ into eq 18, to yield eq 20, by which contributions of NH_2Cl and HOCl to As(III) loss can be modeled together.

$$[\text{As(III)}] = [\text{As(III)}]_0 \, e^{(-(k''_{\text{app},NH_2Cl}[NH_2Cl] + k''_{\text{app,FAC}}[FAC]_{eq})\ t)} \quad (20)$$

As shown by the solid lines in Figure 2d, eq 20 yielded predictions that are in very good accord with measured As(III) loss in LZ1 and LZ20 waters, illustrating that the NH_2Cl–HOCl equilibrium plays a significant role in governing As(III) loss in the presence of excess NH_2Cl. However, predictions obtained for PV water by eq 20 still deviated substantially from measured As(III) losses (Figure 2d). The reason for these discrepancies is presently unknown.

Ozonation. Figure 3a depicts measured As(III) losses for various O_3 doses in LZ, YP, and PV waters. A dose of only 0.25 mg/L O_3 (5.2×10^{-6} M) was sufficient to achieve >99% loss of 50 μg/L As(III) (6.7×10^{-7} M) in LZ and YP waters. Comparable oxidation of 50 μg/L As(III) was also achieved in PV water at a relatively low O_3 dose (0.8 mg/L O_3, or 1.7×10^{-5} M) (Figure 3a), because O_3, in contrast to FAC, reacts very slowly with NH_3 ($k''_{app,O_3,NH_3} = 0.2$ M^{-1} s^{-1} at pH 7.3 (*29*)). The observation that more O_3 than FAC (on a molar basis) is required to achieve comparable oxidation of As(III) in LZ and YP waters (Figures 2a and 3a) can be attributed to the higher reactivity of O_3 toward DOM, which results in comparably more rapid O_3 loss to side-reactions with water matrix constituents.

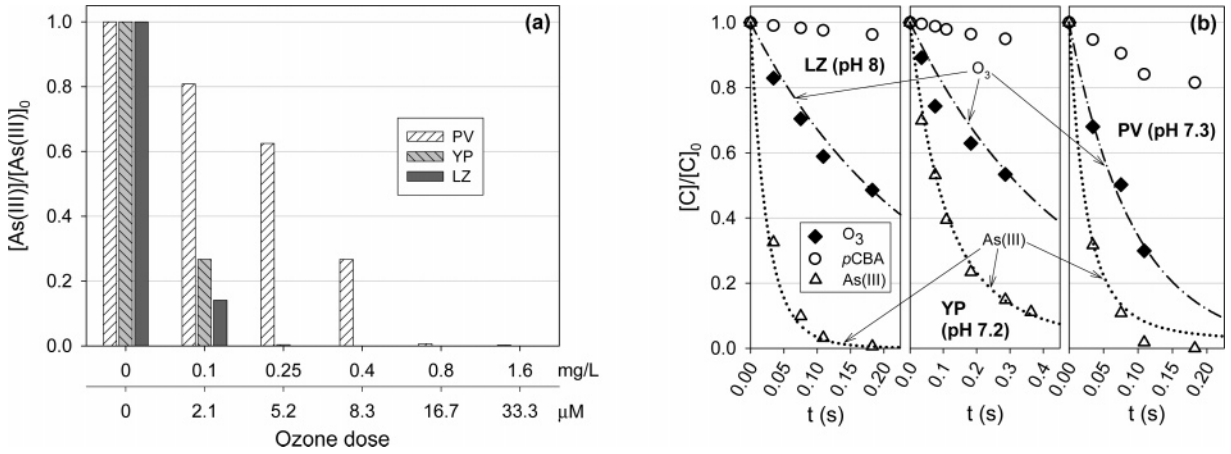

FIGURE 3. As(III) oxidation during ozonation of real waters spiked with 50 μg/L As(III) (6.7×10^{-7} M) (water quality data in Table 2). (a) As(III) loss for various O_3 doses within real waters included in this study, in batch at 25 (±0.5) °C, (b) time-resolved As(III) loss within LZ water ($[O_3]_0 = 0.25$ mg/L (5.2×10^{-6} M), 23 (±2) °C), YP water ($[O_3]_0 = 0.25$ mg/L (5.2×10^{-6} M), 23 (±2) °C), and PV water ($[O_3]_0 = 1$ mg/L (2.1×10^{-5} M), 23 (±2) °C). Symbols refer to measurements, lines to model predictions.

Figure 3b, depicting time-resolved measurements of O_3 and As(III) losses in LZ, YP, and PV waters, illustrates that $t_{1/2,O_3}$ is less than 0.33 s in LZ and YP waters, whereas $t_{1/2,FAC}$ exceeds 1.8 s for the same waters (Figure 2b). Molar-equivalent doses of FAC and O_3, therefore, resulted in similar rates of As(III) oxidation within these waters, even though the magnitude of k''_{app,O_3} exceeds that of $k''_{app,FAC}$ by a factor of 5−15 at circumneutral pH. Figure 3b also shows that O_3 loss is more rapid in PV water than in LZ or YP waters, due to the higher DOC concentration in PV water. This is consistent with the comparably lower efficiency of As(III) oxidation by O_3 in PV water (Figure 3a). Furthermore, Figure 3b shows that the rate of As(III) loss is significantly faster in LZ water than in YP water, and approximately equivalent to the rate of As(III) loss in PV water, even though the latter was dosed with four times as much O_3. This can be attributed in part to the higher pH of LZ water; that is, k''_{app,O_3} is 9.4×10^6 M^{-1} s^{-1} at pH 8 (LZ water), compared to 2.0×10^6 M^{-1} s^{-1} at pH 7.2 (YP water) and 2.4×10^6 M^{-1} s^{-1} at pH 7.3 (PV water).

Hydroxyl radicals (·OH) − generated by autocatalytic O_3 decomposition or by direct reactions of O_3 with water matrix constituents (*30,31*) − also react rapidly with As(III) ($k''_{\cdot OH,As(OH)_3} = 8.5\ (\pm 0.9) \times 10^9\ M^{-1}\ s^{-1}$ (*32*)). *p*-Chlorobenzoic acid (*p*CBA), which reacts rapidly with ·OH, but is nonreactive toward O_3, was used as an in situ probe (*33*) to evaluate the importance of ·OH−As(III) reactions during ozonation of each real water. The *p*CBA losses depicted in Figure 3b show that ·OH was generated in measurable yield within each system. However, calculated contributions of ·OH to observed As(III) losses were very low (i.e., <5% of total observed loss for LZ and YP waters, and <10% for PV water, see Supporting Information, Text S7 for a detailed discussion). Time-resolved measurements of As(III) losses in these waters were, therefore, modeled by considering only O_3−As(III) reaction kinetics (via eq 15, with O_3 terms substituted for FAC terms). The close agreement of model predictions with experimental data confirms that As(III) loss was dominated by direct reactions with O_3 (Figure 3b).

Implications for As(III) Oxidation during Full-Scale Drinking Water Treatment. As demonstrated here and in prior work (*10*), oxidant-scavenging matrix constituents such as NH_3 and DOM can lower the efficiency of As(III) preoxidation processes. Fe(II), which reacts very rapidly with FAC and O_3 at pH ≤ 2 (*34, 35*), may represent another important oxidant scavenger in such waters, though FAC−Fe(II) and O_3−Fe(II) reaction kinetics must be measured at circumneutral pH to permit quantitative evaluation of its potential influence on chlorination or ozonation processes.

When oxidant-scavenger concentrations are relatively low, their influence on As(III) oxidation efficiency during chlorination or ozonation processes will likely be offset by the extremely fast kinetics of FAC−As(III) and O_3−As(III) reactions. However, high scavenger concentrations may substantially impair As(III) oxidation efficiency (Figures 2a and 3a). Proper selection of oxidants can minimize matrix effects in the latter case. For example, ozonation will generally be preferable to chlorination for oxidation of As(III) in waters containing high NH_3 concentrations (e.g., PV water), because O_3 reacts slowly with NH_3. In comparison, chlorination is likely to prove more efficient than ozonation for As(III) oxidation in waters lacking NH_3, because FAC typically reacts more slowly than O_3 with DOM over time-scales relevant to FAC−As(III) reactions (Figures 2b and 3b).

In waters with high oxidant scavenging rates, As(III) oxidation efficiencies will also be highly sensitive to mixing efficiency during oxidant application (Figure 2c). The high sensitivity of FAC−As(III) and O_3−As(III) reaction kinetics to pH (Figure 1) indicates that pH control may also play an important role in As(III) oxidation efficiency. Careful attention to these considerations will facilitate optimization of oxidant dose when As(III) oxidation must be balanced with constraints such as disinfection byproduct formation.

In an optimized chlorination or ozonation process, complete preoxidation of As(III) should generally be achievable at oxidant doses for which disinfection byproduct formation will be minimal. For example, THM and NDMA formation potentials in YP and PV waters are known to be far below WHO, EU, and USEPA limits at the FAC doses required to achieve full As(III) oxidation within these waters during the present investigation (*13*). Bromate formation during ozonation of these waters is also expected to be low, because YP water contains low Br^- concentrations (i.e., <30 μg/L), and PV water contains high NH_3 concentrations, which will substantially suppress bromate formation by scavenging HOBr generated by reaction of O_3 with Br^- (*36*).

NH_2Cl formed during chlorination of ammoniacal waters will likely only have appreciable effect on As(III) fate in special cases; for example, if source waters undergo limited or no treatment prior to chlorination, and insufficient FAC is added to directly oxidize As(III) during chlorination. Although the direct NH_2Cl−As(III) reaction may result in minimal As(III) oxidation after chlorination, indirect NH_2Cl-mediated oxidation reactions can yield substantial As(III) oxidation within

such systems over reaction times of several hours (e.g., within disinfection contact chambers or distribution networks), as illustrated in Figure 2d.

Acknowledgments

M.C.D. and N.D.V. contributed equally to this work. Travel scholarships and financial support for N.D.V. and V.C.L. were obtained from the Swiss Agency for Development and Cooperation (SDC), in the framework of the Swiss-Vietnamese project ESTNV (Environmental Science and Technology in Northern Vietnam). M.C.D. gratefully acknowledges financial support from a U.S. National Science Foundation Graduate Research Fellowship. The authors thank Elisabeth Salhi, Caroline Stengel, and Sebastien Meylan for their technical assistance. Willem Koppenol is acknowledged for support in obtaining stopped-flow measurements of As(III)-O_3 reaction kinetics. The authors also thank Stephan Hug, Linda Roberts, Olivier Leupin, Marc-Olivier Buffle, and Gretchen Onstad for many helpful discussions. The Hanoi Water Works Company is acknowledged for assistance in obtaining water samples from Hanoi.

Supporting Information Available

Tables and figures addressing experimental methods and modeling approaches, water sample sources and procurement, reaction orders and stoichiometries, As(III)-$NHCl_2$ reaction kinetics, and temperature-dependence of As(III)-NH_2Cl reaction kinetics, in addition to reaction kinetics data from which rate constants were determined. This material is available free of charge via the Internet at http://pubs.acs.org.

Literature Cited

(1) Cullen, W. R.; Reimer, K. J. Arsenic Speciation in the Environment. *Chem. Rev.* **1989**, *89*, 713−764.
(2) Frey, M. M.; Edwards, M. A. Surveying arsenic occurrence. *J. Am. Water Works Ass.* **1997**, *89*, 105−117.
(3) Berg, M.; Tran, H. C.; Nguyen, T. C.; Pham, H. V.; Schertenleib, R.; Giger, W. Arsenic contamination of groundwater and drinking water in Vietnam: A human health threat. *Environ. Sci. Technol.* **2001**, *35*, 2621−2626.
(4) Smith, A. H.; Lingas, E. O.; Rahman, M. Contamination of drinking-water by arsenic in Bangladesh: A public health emergency. *Bull. W. H. O.* **2000**, *78*, 1093−1103.
(5) *Guidelines for Drinking-water Quality*; 3rd ed.; World Health Organization: Geneva, Switzerland, 2004; Vol. 1.
(6) Hering, J. G.; Chiu, V. Q. Arsenic occurrence and speciation in municipal groundwater-based supply system. *J. Environ. Eng., ASCE* **2000**, *126*, 471−474.
(7) Council Directive 98/83/EC of 3 November 1998 on the quality of water intended for human consumption. *Off. J. Eur. Communities* **1998**, *41*, 32−54.
(8) National Primary Drinking Water Regulations. *Code of Federal Regulations,* Part 141, Title 40, 2001, http://www.epa.gov/epahome/cfr40.htm.
(9) *Technologies and Costs for Removal of Arsenic from Drinking Water*, United States Environmental Protection Agency—Office of Water: Washington, DC, 2000 (http://www.epa.gov/safewater/ars/treatments_and_costs.pdf).
(10) Ghurye, G.; Clifford, D. As(III) oxidation using chemical and solid-phase oxidants. *J. Am. Water Works Assoc.* **2004**, *96*, 84−96.
(11) Leupin, O. X.; Hug, S. J.; Badruzzaman, A. B. M. Arsenic removal from Bangladesh tube well water with filter columns containing zerovalent iron filings and sand. *Environ. Sci. Technol.* **2005**, *39*, 8032−8037.
(12) McArthur, J. M.; Ravenscroft, P.; Safiulla, S.; Thirlwall, M. F., Arsenic in groundwater: Testing pollution mechanisms for sedimentary aquifers in Bangladesh. *Water Resour. Res.* **2001**, *37*, 109−117.
(13) Duong, H. A.; Berg, M.; Hoang, M. H.; Pham, H. V.; Gallard, H.; Giger, W.; von Gunten, U. Trihalomethane formation by chlorination of ammonium- and bromide-containing groundwater in water supplies of Hanoi, Vietnam. *Water Res.* **2003**, *37*, 3242−3252.
(14) *Standard Methods for the Examination of Water and Wastewater*, 20th ed.; APHA, AWWA, WPCF: Washington DC, 1998.
(15) Kumar, K.; Day, R. A.; Margerum, D. W. Atom-transfer redox kinetics: General-acid-assisted oxidation of iodide by chloramines and hypochlorite. *Inorg. Chem.* **1986**, *25*, 4344−4350.
(16) Bader, H.; Hoigné, J. Determination of ozone in water by the indigo method. *Water Res.* **1981**, *15*, 449−456.
(17) Leitzke, A.; Reisz, E.; Flyunt, R.; von Sonntag, C. The reactions of ozone with cinnamic acids: formation and decay of 2-hydroperoxy-2-hydroxyacetic acid. *J. Chem. Soc., Perkin Trans. 2* **2001**, 793−797.
(18) Sadiq, M.; Zaidi, T. H.; Mian, A. A. Environmental behavior of arsenic in soils—theoretical. *Water Air Soil Pollut.* **1983**, *20*, 369−377.
(19) Lide, D. R., Ed. *CRC Handbook of Chemistry and Physics*, 82nd ed.; CRC Press: Boca Raton, FL, 2001.
(20) Stumm, W.; Morgan, J. J. *Aquatic Chemistry*, 3rd ed.; John Wiley and Sons: New York, 1996.
(21) Fogelman, K. D.; Walker, D. M.; Margerum, D. W. Non-metal redox kinetics: hypochlorite and hypochlorous acid reactions with sulfite. *Inorg. Chem.* **1989**, *28*, 986−993.
(22) Gerritsen, C. M.; Margerum, D. W. Non-metal redox kinetics: hypochlorite and hypochlorous acid reactions with cyanide. *Inorg. Chem.* **1990**, *29*, 2757−2762.
(23) Qiang, Z.; Adams, C. D. Determination of monochloramine formation rate constants with stopped-flow spectrophotometry. *Environ. Sci. Technol.* **2004**, *38*, 1435−1444.
(24) Yiin, B. S.; Walker, D. M.; Margerum, D. W. Nonmetal redox kinetics: general-acid-assisted reactions of chloramine with sulfite and hydrogen sulfite. *Inorg. Chem.* **1987**, *26*, 3435−3441.
(25) Margerum, D. W.; Schurter, L. M.; Hobson, J.; Moore, E. E. Water Chlorination Chemistry: Nonmetal Redox Kinetics of Chloramine and Nitrite Ion. *Environ. Sci. Technol.* **1994**, *28*, 331−337.
(26) Hoigné, J. In *The Handbook of Environmental Chemistry;* Hrubec, J., Ed.; Springer-Verlag: Berlin, Germany, 1998; pp 83−141.
(27) Liu, Q.; Schurter, L. M.; Muller, C. E.; Aloisio, S.; Francisco, J. S.; Margerum, D. W. Kinetics and mechanisms of aqueous ozone reactions with bromide, sulfite, hydrogen sulfite, iodide, and nitrite ions. *Inorg. Chem.* **2001**, *40*, 4436−4442.
(28) Gray, E. T., Jr.; Margerum, D. W.; Huffman, R. P. In *Organometals and Organometalloids, Occurrence and Fate in the Environment;* Brinkman, F. E., Bellama, J. M., Eds.; American Chemical Society: Washington, D. C., 1978; pp 264−277.
(29) Hoigné, J.; Bader, H. Ozonation of water: Kinetics of oxidation of ammonia by ozone and hydroxyl radicals. *Environ. Sci. Technol.* **1978**, *12*, 79−84.
(30) Buffle, M.-O.; Schumacher, J.; Salhi, E.; von Gunten, U. Measurement of the initial phase of ozone decomposition in water and wastewater by means of a continuous quench flow system: Application to disinfection and pharmaceutical oxidation. *Water Res.* **2006**, in press.
(31) von Gunten, U. Ozonation of drinking water: Part I. Oxidation kinetics and product formation. *Water Res.* 2003, *37*, 1443−1467.
(32) Klaening, U. K.; Bielski, B. H. J.; Sehested, K. Arsenic(IV)—a pulse-radiolysis study. *Inorg. Chem.* **1989**, *28*, 2717−2724.
(33) Elovitz, M. S.; von Gunten, U. Hydroxyl radical/ozone ratios during ozonation processes. I. The R_{ct} concept. *Ozone: Sci. Eng.* **1999**, *21*, 239−260.
(34) Conocchioli, T. J.; Hamilton, E. J.; Sutin, N. Formation of Iron-(IV) in Oxidation of Iron(II). *J. Am. Chem. Soc.* **1965**, *87*, 926−927.
(35) Løgager, T.; Holcman, J.; Sehested, K.; Pedersen, T. Oxidation of Ferrous-Ions by Ozone in Acidic Solutions. *Inorg. Chem.* **1992**, *31*, 3523−3529.
(36) Pinkernell, U.; von Gunten, U. Bromate minimization during ozonation: Mechanistic considerations. *Environ. Sci. Technol.* **2001**, *35*, 2525−2531.

Received for review December 13, 2005. Revised manuscript received March 7, 2006. Accepted March 10, 2006.

ES0524999